Title: The memory of airway epithelium damage in smokers and COPD patients.

Authors: François M. Carlier[1,2], MD; Bruno Detry[1]; Marylène Lecocq[1]; Amandine M. Collin[1], PhD; Stijn E. Verleden[3], PhD; Claudia M. Stanciu-Pop[4], MD; Wim Janssens[3], MD PhD; Jérôme Ambroise[5], PhD; Bart M. Vanaudenaerde[3], MD PhD; Sophie T. Gohy[1,6], MD PhD; and Charles Pilette[1,6*], MD PhD.

Affiliations:

[1]Pole of Pneumology, ENT, and Dermatology, Institute of Experimental and Clinical Research, Université Catholique de Louvain, Brussels, Belgium

[2]Department of Pneumology, CHU Mont-Godinne UCL Namur, Yvoir, Belgium

[3]Department of chronic diseases, metabolism and ageing, Katholieke Universiteit Leuven, Leuven, Belgium

[4]Department of Pathology, CHU Mont-Godinne UCL Namur, Yvoir, Belgium

[5]Centre de Technologies Moléculaires Appliquées, Institute of Experimental and Clinical Research, Université catholique de Louvain, Brussels, Belgium;

[6]Department of Pneumology, Cliniques Universitaires St-Luc, Brussels, Belgium

*__Corresponding author__

Charles Pilette, MD PhD

Pole of Pneumology, ENT, and Dermatology

Institute of Experimental and Clinical Research

Université Catholique de Louvain

Tour Claude Bernard +5

Avenue Hippocrate, 54

Bte B1.54.04

1200 Brussels

Belgium

Phone : +3227649449

Fax : +3227649440

charles.pilette@uclouvain.be

Author contributions

F.M.C. performed experiments, most data analysis, co-supervised the experimental design and wrote the manuscript. B.D. helped with cell cultures and samples collection. M.L. processed samples, designed PCR primers and performed some PCR. S.E.V. and C.M.S. collected and provided samples. W.J. and B.M.V. revised the manuscript. J.A. performed single cell RNA sequencing analysis. A.M.C. helped with cell cultures. S.T.G. helped with manuscript redaction and revision. C.P. supervised the design of the study and the writing of the manuscript.

Acknowledgements. The authors would like to thank J. Van Snick for his help with IL-6 ELISA, V. Lacroix, B. Rondelet and D. Hoton for providing surgical tissue, A. Daumerie for technical advices, M. de Beukelaer and Ch. Fregimilicka for their help with samples processing, and the IREC Pole of Microbiology (UCLouvain, Brussels, Belgium) for sharing their molecular biology facility.

Sources of support. This work was supported by the Fondation Mont-Godinne, Belgium, grant to FC (N°FMG-2015-BC01, FMG-2016-BC01, and FMG-2017-BC01) by the Fonds National de Recherche Scientifique (FNRS), Belgium, grant to FC (N°1.L505.18) and to CP (N°1.R016.16 and 1.R016.18). Funders were not involved in study design, data collection, data analysis, interpretation, or writing of the manuscript.

Competing interests. The authors have nothing to disclose.

48 **Correspondence and requests for materials** should be addressed to C.P.

49 (charles.pilette@uclouvain.be)

50 **Running title:** Memory of airway epithelium pathology in COPD

51 **Word count**

52

Abstract.

Background. Chronic obstructive pulmonary disease (COPD) is a devastating lung disease, representing the third cause of mortality worldwide. In COPD, the bronchial epithelium displays several structural and functional abnormalities involving barrier integrity, polarity, cell differentiation and epithelial-to-mesenchymal transition, as well as inflammation. Although COPD is currently considered as an irreversible disease, the (ir)reversible nature of those changes *ex vivo* remains poorly known.

Methods. The persistence of COPD epithelial features was assessed in very long-term (10 weeks) primary cultures of air/liquid interface (ALI)-reconstituted airway epithelium from non-smoker controls, smoker controls, and COPD patients. The role of inflammation in promoting this phenotype was also explored by stimulating ALI cultures with a cytokine mix of TNF-α, IL-6 and IL-1β.

Results. Almost all epithelial defects (barrier dysfunction, impaired polarity, lineage abnormalities) observed in smokers and COPD persisted *in vitro* up to week 10, except IL-8 release and epithelial-to-mesenchymal transition which declined over time. Cytokine treatment induced COPD-like changes and was able to reactivate epithelial-to-mesenchymal transition in COPD cells.

Conclusions. The airway epithelium from smokers and COPD patients displays a memory of its native state and previous injuries by cigarette smoking, which is multidimensional and sustained for years, therefore probably residing in basal stem cells.

Abstract word count. 200

Key words. COPD, airway epithelium, barrier dysfunction, EMT, inflammation, pIgR

Introduction

Chronic obstructive pulmonary disease (COPD), currently representing the third leading cause of death worldwide (1), is mainly due to cigarette smoking while exposure to other toxics (biomass, occupational, air pollution) and genetic predisposition also play a role (2). It is characterized by a progressive and mostly irreversible airway obstruction related to small airway pathology and destruction of the alveolar walls, referred to as emphysema (3). The irreversible nature of the disease also refers to the relatively modest effects of currently available therapies (4) including inhaled corticosteroids and bronchodilators, none of which targeting the underlying pathways leading to structural remodelling of the lungs.

The bronchial epithelium, as first line barrier against inhaled particles and antigens, is constantly exposed to airborne pollutants. In COPD, the airway epithelium (AE) structure and biology are profoundly altered in terms of barrier function, cell differentiation and epithelial-to-mesenchymal transition (EMT), epithelial polarity, and inflammation.

First, AE barrier function is impaired in COPD (5): while it was shown that cigarette smoke (CS) exposure alone decreases the expression of tight junction proteins (*OCLN1*, *ZO1*)(6), the AE from COPD patients appears more prone to develop barrier dysfunction, as CS extract-exposed COPD human bronchial epithelial cells (HBEC) show decreased E-cadherin and zonula occludens 1 (ZO-1) expression as compared with HBEC from smokers (7). Globally, COPD AE displays increased epithelial permeability, probably favouring microbial invasion and COPD exacerbations, which account for a significant part of COPD morbidity (5, 8, 9).

Second, the COPD bronchial epithelium is characterized by altered lineage differentiation, with hyperplastic and dysfunctional basal cells (10, 11), decreased function and numbers in ciliated cells (12), decreased club cells numbers and club cell secretory protein (SCGB1A1) excretion (13, 14) and hyperplastic goblet cells, the latter being possibly more related to CS than to the

disease *per se* (15). In addition, CS leads to transforming growth factor (TGF)-β-induced EMT that is further enhanced in COPD patients (7) both in large and small airways (16), contributing to subepithelial fibrosis and cancer susceptibility in COPD patients (17). Interestingly, both EMT and altered lineage differentiation of the AE may be reproduced *in vitro*, in the AE reconstituted by 4 week long culture in air/liquid interface (ALI) of HBEC from COPD patients (18, 19).

Finally, epithelial inflammation is a paramount feature in COPD that is thought to represent a major player in the disease pathophysiology (20). In line with the increased presence of intraepithelial neutrophils (21), increased levels in tumor necrosis factor (TNF)-α, interleukin-8/C-X-C Motif Chemokine Ligand 8 (IL-8/CXCL-8) and neutrophils have been observed in sputum from COPD patients (22, 23) and correlate with disease severity (24).

It remains unclear whether structural changes of the AE are persistent in COPD, matching the irreversible nature of the disease *in vivo*. It has been reported that COPD patients who quitted smoking for more than 3,5 years display less goblet cell hyperplasia and squamous metaplasia (25), and that smoking cessation may slightly improve pulmonary function tests (26) and reduce mortality of COPD patients (27). In contrast, smoking cessation does not influence COPD-related increased epidermal growth factor receptor (EGFR) activation (25) and protease activity (28). In COPD, the inflammatory pattern that is shared with 'healthy' smokers is amplified and persists even after smoking cessation (29), although with conflicting data in other studies (26, 29, 30). This study aimed to elucidate whether the AE changes are imprinted in a persistent manner, or whether some changes could be reversible, i.e. questioning the memory retained in epithelial cells from COPD patients (31).

To address this question, the AE was reconstituted in the ALI culture model with primary HBEC from non-smokers, control smokers and COPD patients, and cultured *in vitro* for up to 10 weeks, and the spontaneous evolution of abnormalities was assayed in terms of barrier

function, cell differentiation, EMT, pIgR/SC-related polarity and inflammatory cytokines' production. In addition, it was assessed whether exogenous inflammation may trigger COPD-related changes in this model.

Materials and methods

Study population and lung tissue samples

A series of lung surgical specimens containing large airways was obtained from four different patients groups (non-smokers, smoker controls, mild and moderate COPD and severe to very severe COPD). COPD patients were sorted on basis of their pulmonary function tests, according to the GOLD 2001 classification. Surgical tissue from lobectomies was used for controls and mild or moderate COPD patients undergoing lung surgery for a solitary tumour, while explants were obtained to analyse lung tissue from patients with (very) severe COPD. Patients with any other lung disease than COPD (e.g. asthma, fibrosis) were excluded from the study. All patients received information and signed a written consent to the study protocol, which was approved by the local clinical Ethical committee (reference 2007/19MARS/58 for UCLouvain, S52174 and S55877 for KULeuven). A primary proximal bronchial epithelium was reconstituted *in vitro* from all subjects, and was subjected to mid-term (5 weeks, n=25) or long-term (10 weeks, n=26) culture. Patients' characteristics are shown in Tables 1, S1 and S2.

In vitro reconstitution of primary human bronchial epithelium on ALI culture

A large piece of cartilaginous bronchus was selected from lobectomies or explants, located as far as possible from the tumour site (in the case of lobectomies) and submitted to pronase digestion overnight at 4°C, in order to derive HBEC. HBEC were cultured in flasks in retinoic acid-supplemented Bronchial Epithelial Cell Growth Basal Medium (BEBM, Lonza, Verviers, Belgium) until confluence. Cells were then detached and seeded at a density of 80,000 cells/well on 24-well polyester filter-type inserts (0.4-µm pore size; Corning, Corning, NY) coated with 0.2 mg/ml collagen IV (Sigma-Aldrich, Saint-Louis, MO) until a confluent monolayer was obtained. The culture was then carried out in ALI for 5 (for 25 subjects) or 10 weeks (for 26 subjects). Once in ALI, HBEC were cultured in BEBM:Dulbecco's Modified Eagles Medium

(DMEM) (1:1) medium supplemented with penicillin (100U/ml), streptomycin (100µg/ml) (Lonza), bovine serum albumin (BSA) (1.5 µg/ml), retinoic acid (30ng/ml) (Sigma, Saint-Louis, MO), and BEGM SingleQuotsTM Supplements and Growth Factors (Lonza), including bovine pituitary extract (52µg/ml), insulin (5µg/ml), hydrocortisone (0.5g/ml), transferrin (10µg/ml), epinephrine (0.5µg/ml), epidermal growth factor (0.5ng/ml) and triiodothyronine (3.25ng/ml). Every week during ALI culture, basolateral media were collected, and the apical pole of HBEC was washed with 300µl sterile phosphate-buffered saline (PBS) before centrifugation for 5 minutes at 10,000 g. Transwell inserts were fixed by direct immersion in 4% buffered formaldehyde, before incubation in PBS (pH 7.4) and embedding in paraffin blocks. ALI-HBEC were also processed for gene expression or Western blot analyses (see below).

The 25 samples that underwent 5 weeks ALI culture were submitted or not (control condition) to a pro-inflammatory cytokine cocktail including IL-1β, IL-6, TNF-α, each at 5 ng/ml (Miltenyi Biotec, Germany) in the basolateral compartment following a preliminary titration experiment (10, 5, and 2,5 ng/ml) where no cytotoxicity (release of lactate dehydrogenase < 5%) was shown at 5 ng/ml.

Measurement of the transepithelial electric resistance

Every week and for each sample, the transepithelial electric resistance (TEER) of the reconstituted epithelium was assessed, using the EMD Millipore™ Millicell-ERS Volt-Ohm Meter (Fisher Scientific, Hampton, NH, USA) after transiently filling the apical pole of the cells with sterile PBS. TEER was measured in duplicates and the mean of the measurements was used, after obtained values were corrected according to the resistance of the transwell membrane.

Reverse transcriptase quantitative polymerase chain reaction (RT-qPCR)

RNA extraction, reverse transcription, and RT-qPCR were performed as previously described (32). Total RNA was extracted from reconstituted ALI cultured epithelia using TRIzol reagent (Thermo Fisher Scientific). 500ng of RNA was reverse-transcribed with RevertAid H minus Reverse transcriptase kit with 0.3 µg of random hexamer, 20U of RNase inhibitor and 1mM of each dNTP (Thermo Fisher Scientific, Waltham, MA) following the manufacturer's protocol in a thermocycler (Applied Biosystems, Foster City, CA). The expression levels were quantified by real-time quantitative PCR with the CFX96 PCR (Bio-Rad, Hercules, CA). The reaction mix contained 2.5 µl of complementary desoxyribonucleic acid diluted 10-fold, 200nM of each primer (primers properties are detailed in Table S3) and 2x iTaq UniverSybr Green® Supermix (Bio-Rad) in a final volume of 20 µl. The cycling conditions were 95°C for 3 minutes followed by 40 cycles of 95°C for 5 seconds and 60°C for 30 seconds. To control the specificity of the amplification products, a melting curve analysis was performed. The copy number was calculated from the standard curve. Data analysis was performed using Bio-Rad CFX software (Bio-Rad). Expression levels of target genes were normalized to the geometric mean of the values of 3 housekeeping genes (RPL27, RPS13, RPS18).

Western blot assays

HBEC lysates were analysed by Western blot as previously described (33) except for band revelation (see below). Cells were lyzed with 150µl of Laemmli's sample buffer containing 0.7M 2-mercaptoethanol (Sigma-Aldrich) and lysates were stored at -20°C. After thawing, samples were heated at 100°C for 5 minutes, loaded in a SDS-PAGE gel before migration at 100V for 15 minutes and then at 180V for 50 minutes. Cell proteins were transferred onto a nitrocellulose membrane (Thermo Fisher Scientific) at 0.3A for 2 hours 10 minutes at RT. The membranes were blocked with 5% w/v BSA (Sigma-Aldrich) in Tris-buffered saline with 0.1% Tween 20 (Sigma-Aldrich) for 1 hour at RT, then washed and incubated overnight at 4°C with a primary antibody according to the target protein (see Table S4 listing used primary and

secondary antibodies). Membranes were then incubated for 1 hour at room temperature (RT) with horseradish peroxidase (HRP)-conjugated secondary anti-rabbit (Cell Signalling, Danvers, MA) or anti-mouse (Sigma) IgG. Immunoreactive bands were revealed by chemiluminescence (GE Healthcare, Pittsburgh, PA), detected by Chemidoc XRS apparatus (Bio-Rad) and quantified using the Quantity One software (Bio-Rad).

Sandwich enzyme-linked immunosorbent assay (ELISA) for SC, IL-8/CXCL-8 and IL-6

SC concentration was determined in apical washes by sandwich ELISA, as previously described (13, 33). Basolateral IL-8/CXCL8 and IL-6 release were assessed by sandwich ELISA, following manufacturer's instructions (Biotechne, Minneapolis, MN). Briefly, 96-well plates were first coated overnight, at 4°C, with anti-IL-8/CXCL8, -IL-6, and -SC antibodies diluted in bicarbonate buffer (pH 9,6). Then, after blocking with 1% w/v BSA in phosphate-buffered saline for 90 min at 37°C, HBEC apical washes (for SC) or basolateral supernatants (for IL-8/CXCL-8 and IL-6) were incubated for 60 min at 37°C, along with standard samples. Detection was performed with a first incubation with the corresponding biotinylated antibody (anti-fibronectin, -SC, -IL-8/CXCL-8 or -IL-6), followed by a second incubation with HRP-linked anti-mouse IgG, for 1 h each. Revelation was performed with 3,3',5,5'-tetramethylbenzidine (TMB, Fisher) and stopped with H_2SO_4 1.8 M.

Direct ELISA for fibronectin

Fibronectin basolateral release was assessed by direct ELISA as previously described (19, 34). HBEC basolateral washes and fibronectin standard were coated in plates with bicarbonate buffer overnight (pH 9,6), at 4°C. After blocking with 1% w/v BSA in phosphate-buffered saline for 90 min at 37°C, detection was performed with a first incubation with mouse anti-fibronectin, followed by a second incubation with HRP-linked anti-mouse IgG, for 1 h each. Revelation was performed with TMB and stopped with H_2SO_4 1.8 M."

225 **Statistical analysis**

226 Results were analysed with JMP® Pro, Version 14 (SAS Institute Inc., Cary, NC, USA) and
227 GraphPad Prism version 8.0.2 for Windows (GraphPad Software, La Jolla, CA, USA), and were
228 expressed as medians and interquartile ranges unless otherwise stated. p-values < 0.05 were
229 considered statistically significant.

230

Results

Barrier and junctional properties in the COPD vs control AE

As physical barrier constitutes a first-line defence provided by the AE, it was assessed whether it was impaired in COPD by measuring the transepithelial electric resistance (TEER) of ALI-reconstituted primary AE cultured for 5 weeks (n_1=51 patients) or up to 10 weeks (n_2=26 patients). According to their smoking status and lung function (GOLD 2001 classification), the study population was divided into 4 groups: non-smoker controls (NS; n_1=10 for 5 weeks and n_2=5 for 10 weeks), smoker controls (Smo; n_1=15 and n_2=7), mild and moderate COPD (COPD GOLD 1-2; n_1=13 and n_2=7) and severe and very severe COPD (COPD GOLD 3-4; n_1=13 and n_2=7). The characteristics of the complete study population are summarized in Table 1, and detailed analysis of separate populations is provided in Tables S1 and S2.

The reconstituted AE from COPD patients displayed substantially decreased TEER as compared with that of non-smoker controls, and to a lesser extent with that of smoker controls (Figure 1). In addition, smoker controls AE also showed decreased TEER compared with that of non-smoker controls. This defect appeared as early as at the first week ALI culture, and was progressively more prominent over time (Figure 1A-D), persisting up to 10 weeks (Figure 1H). Between 2 and 10 weeks ALI culture, TEER inversely correlated modestly but significantly with the disease severity witnessed by the forced expiratory volume in one second (FEV1) (Figure 1E-G).

To elucidate the molecular substratum of this long-lasting barrier disruption, gene and protein expression of major components of the tight and adherens junctions was assayed, namely claudin-1 (*CLDN1*), E-cadherin (*CDH1*), occludin (*OCLN*) and ZO-1/tight junction protein 1 (*TJP1*). Although no difference was observed between groups regarding gene expression (Figure S1), protein expression of E-cadherin was reduced in COPD as compared with non-

smoker controls after 1 and 3 weeks ALI culture, but not at 6 and 9 weeks (Figure 2A-D) and that of occludin was decreased in smokers and COPD AE at 3, 6 and 9 weeks and inversely correlated with the disease severity, assessed by the FEV1 (Figure 2E-H). Figure 2 I-J shows representative blots for E-cadherin (at 1 and 3 weeks), and occludin (at 6 and 9 weeks).

These data globally depict a barrier and junctional defect that is engaged in smokers, that further aggravates in COPD (in relation to disease severity) and that appears persistent in prolonged *in vitro* culture.

Epithelial differentiation of the COPD vs control AE

In order to assess the persistence of the abnormal programming of epithelial differentiation in COPD, specific markers and transcription factors of basal, intermediate, goblet, club and ciliated cells were assayed in long-term ALI cultures.

Epithelial pre-differentiation

Gene expression of MYB Proto-Oncogene (*MYB*), a recently described marker of early differentiation of basal cells (37), was significantly decreased up to 8 weeks in smokers- and COPD-derived AE as compared with non-smokers (Figures 3A and S2A). In addition, the expression of *MYB* at 1, 2, 4 and 8 weeks correlated with disease severity in terms of FEV1 (Figures 3D and S2A).

Differentiation towards ciliated cells

As the COPD AE also classically displays reduced numbers of ciliated cells, it was next assessed whether this defect persisted in long-term ALI cultures by measuring the gene expression of Forkhead Box J1 (*FOXJ1*), a transcription factor involved in the commitment towards ciliated cells, and of the dynein axonemal intermediate chain 1 (*DNAI1*), a marker of terminal differentiation of ciliated cells. Smokers- and COPD-derived cultures displayed a

marked and persisting decrease in both genes as compared with non-smoker controls (Figures 3B-C and S2B-C). This decrease significantly correlated with disease severity (assessed by the FEV1) at 1, 2, and 8 weeks of ALI culture (Figures 3D and S2B-C).

Differentiation towards goblet cells

Recent studies have shown that goblet cell hyperplasia is more closely related to tobacco smoking and to chronic bronchitis rather than airway obstruction and COPD *per se* (35). In our study, we assessed the gene expression of SAM Pointed Domain Containing ETS Transcription Factor (*SPDEF*) and Forkhead Box A3 (*FOXA3*), two transcription factors inducing the differentiation towards goblet cells (36-38). On one hand, *SPDEF* expression was increased in smoker controls' AE (and in COPD AE, although to a lesser, non-significant extent), as compared with that of non-smokers (Figures 3E and S2D). This was also observed by a longitudinal analysis comparing smoker controls and non-smokers, this upregulation persisting up to 8 weeks. In addition, *SPDEF* expression was decreased in smokers who quitted smoking for more than 4 years as compared with active smokers and ex-smokers with a smoking cessation of less than 4 years (Figure 3F and S3E). On the other hand, longitudinal analysis showed that *FOXA3* was also upregulated in smoker controls as compared with non-smokers and mild and moderate COPD (Figure S2F). These data further show that goblet cell hyperplasia relates to smoking and demonstrate that this feature persists over time *in vitro*.

Epithelial-to-mesenchymal transition of the COPD AE

EMT is a physiological process that allows tissue repair, but that is abnormally activated in COPD, inducing subepithelial fibrosis and favouring cancer (17). Thus, EMT protein markers (vimentin, fibronectin) were assessed in long-term ALI cultures. Increased vimentin content was observed at 1, 3 and 5 weeks, but no more at 8 weeks, in (very) severe COPD AE compared with non-smoker controls (Figure 4A-B), as well as in smokers and mild/moderate COPD AE

at 1 week. Accordingly, mild/moderate and (very) severe COPD AE displayed increased fibronectin release in the basolateral medium up to 4 and 7 weeks, respectively, as compared with non-smokers, while it was significantly increased in control smokers at 1 week only (Figure 4C). No difference was seen anymore at 10 weeks. No striking difference was seen for vimentin gene expression (*VIM*, Figure S3). These data show EMT features that are progressively vanishing, after 7 to 10 weeks in COPD and more rapidly in smokers, as summarized in Figure 4D.

Polarity and pIgR/SC expression in the COPD vs control AE

Firstly, smokers- and COPD-derived AE released less apical SC than non-smokers, from 2 weeks of ALI culture until 8 weeks (Figure 5A). In addition, apical SC levels (from 2 to 9 weeks) inversely correlated with disease severity (Figure 5B and S4A). When analysed longitudinally over 10 weeks, this decrease was more pronounced in (very) severe COPD as compared with smoker controls and mild/moderate COPD (Figure 5B). Secondly, the (very) severe COPD AE displayed decreased *PIGR* gene expression throughout the long-term cultures compared with the other groups. Although this was not significant on isolated time points (Figure 5C and S4B), longitudinal data analysis demonstrated decreased PIGR gene expression in (very) severe COPD AE as compared with non-smokers, smoker controls, and mild/moderate COPD AE (Figure 5C). In addition, considering that epithelial differentiation is completed at 5 weeks, we show that the acquisition of pIgR at the protein level was delayed in COPD AEs compared with controls, as depicted in Figure 5D. Figure 5D also shows representative blots of pIgR expression kinetics (1-5 weeks) in ALI-AE from a non-smoker (upper gel) and a very severe COPD patient (lower gel).

These data show that airway epithelial polarity, witnessed by the pIgR/SC expression, is deeply impaired in COPD in a persistent manner.

Inflammatory cytokine production by the COPD vs control AE

As inflammation constitutes a cardinal feature of the COPD epithelium (20, 39), epithelial production of IL-8/CXCL-8 and IL-6 was next assayed in the reconstituted AE. A trend for increased *CXCL8* gene expression was seen in smokers and COPD groups, that was more marked from 1 to 4 weeks ALI culture (Figure S5A). Accordingly, IL-8/CXCL-8 release was strongly increased in smokers- and COPD-derived AE at 1, 2 and 4 weeks as compared with non-smokers, whilst this difference disappeared afterwards (Figure 6A). Although no difference was observed in the expression of the *IL6* gene (Figure S5B), the production of IL-6 in the basolateral medium was increased in smokers and COPD ALI-AE. In contrast to IL-8, IL-6 upregulation persisted over time (up to 10 weeks), both in smokers and COPD (Figures 6B).

Exogenous inflammation induces COPD-like features in the AE

As epithelial inflammation is thought to contribute to epithelial pathology in COPD (20, 40), it was assessed whether exogenous inflammation could promote COPD-like changes in the AE by supplementing the culture medium with IL-6, TNF-α and IL-1β (all at 5ng/ml) for 5 weeks. These cytokines are relevant to human COPD pathogenesis, as besides abovementioned CXCL-8/IL-8 and IL-6, TNF-α and IL-1β are also increased in COPD (22, 41), even though their concentration did not reach the detection threshold in our culture supernatants (not shown).

First, TEER was dramatically decreased upon the inflammatory condition. This was already observed at 1 week ALI culture, but was more pronounced in the next weeks (Figure 7A). Cytokine-exposed cultures displayed similar values irrespectively of the original phenotype, with TEER values comprised between 300 and 600 Ω/cm² between 2 and 5 weeks, possibly indicating a maximal effect on barrier (dys)function at the used concentrations.

Second, cultures that were exposed to inflammatory cytokines displayed sharper EMT features, with increased fibronectin release at 1, 2 and 4 weeks (Figure 7B). Interestingly, this induction that was not observed in non-smokers' AE was strikingly upregulated in COPD as compared to controls (Figure 7C). This phenomenon was confirmed by assessing vimentin expression (Figure 7D). These results show that the cultured AE from COPD patients, whilst losing its intrinsic EMT features, remains prone to develop EMT upon exposure to inflammatory cytokines.

Third, cytokine-induced inflammation altered epithelial polarity assayed through the pIgR/SC system, as SC apical release was decreased in cytokine-exposed AE from non-smoker controls, smoker controls and mild-to-moderate COPD (Figure 7E). This was not observed in (very) severe COPD AE, probably because the pIgR/SC system is already severely impaired in this group.

In conclusion, exogenous inflammation was able to induce COPD-like changes such as barrier dysfunction, EMT and altered polarity in the AE from non-smoker and smoker controls. In addition, the COPD-derived AE remained prone to develop EMT features upon inflammatory condition.

Discussion

This study demonstrates, by using long-term cultures of the ALI-reconstituted human AE from well-characterized COPD and control patients, that the AE retains its native abnormalities for prolonged periods of time (e.g. barrier dysfunction, altered cell differentiation, and impaired polarity) whereas some features (IL-8 upregulation, EMT) disappear. It also demonstrates that inflammation driven by TNF-α, IL-6 and IL-1β, may induce a COPD-like phenotype, and reactivates EMT programming in the diseased (COPD) epithelium in a much wider extent than in the normal epithelium.

COPD is a chronic and progressive disease that is developed upon repeated injury of the airway epithelial-mesenchymal unit by toxics, leading to activation and remodelling of the AE, and ultimately to airway obstruction. The airflow limitation is not or poorly reversible to current inhaled bronchodilators and anti-inflammatory drugs. It has been shown that COPD patients who quitted smoking may benefit from decreases in mortality (27), respiratory symptoms and lung function decline as compared with active smokers (26, 42, 43). They also display reduced AE remodelling and goblet cell hyperplasia when smoking cessation exceeds 3,5 years (25), as well as improvements in nasal mucociliary clearance (44). In contrast, no change was observed following smoking cessation regarding axonemal abnormalities in ciliated cells (45) or airway mucosal inflammation (29), sputum IL-8/CXCL-8 (46) and sputum neutrophils (28, 46).

In this study, we assessed whether the irreversible nature of the disease is imprinted in the AE in such a way that aberrant features of the native epithelium persist in long-term cultures, independently of signals provided by mesenchymal cells and surrounding leucocytes. The ALI model was used, as it was previously shown to recapitulate, at least to some extent, the native phenotype (18, 19, 47-49). We prolonged the culture up to 10 weeks, an unusually long duration in this model, that had not yet been reported so far in COPD.

A major abnormality that persists in the cultured smokers' and COPD AE is the barrier and junctional defect. Thus, the AE from smokers displays a persistent TEER decrease as compared with non-smokers, which was associated with decreased protein levels of E-cadherin and occludin, key components of adherens and tight junctions, respectively. This defect was observed in line with a previous study showing that CS exposure leads to disruption of apical junctional complexes (50) and in a persistent manner, up to 9 weeks of culture for occludin. In addition, those changes in TEER and occludin/E-cadherin expression were further downregulated according to the presence and the severity of the COPD. Gene expression for

main apical junctional complex components (*TJP1*, *OCLN*, *ECAD*, *CLDN11*, Figure S1) did however not differ across the groups, suggesting post-transcriptional regulation.

In line with the requirement of the integrity of apical junctional complexes to ensure baso-apical epithelial polarity (51), our study shows that AE polarity is persistently impaired in COPD. The pIgR/SC system, that allows baso-apical transcytosis of polymeric immunoglobulins (mostly dimeric IgA) across the epithelium and constitutes a marker of epithelial polarity, was previously shown to be defective in COPD, both *in situ* in surgical tissue and *in vitro* in ALI-HBEC evaluated at 2 weeks (48). The present study demonstrates that this impairment persists over time, with decreases in the apical release of SC and in the gene expression of *PIGR*, that is observed in very severe COPD (Figures 5 and S4). In addition, the dynamics of optimal pIgR protein expression was delayed in COPD AE (Figure 5D). Interestingly, those data are contrasting with previous findings in asthma where it was shown that pIgR is also downregulated but this defect, which was related to IL-4R activation, does not persist in ALI culture of the AE from asthma patients (52), suggesting distinct mechanisms driving epithelial pathology in asthma and COPD.

Aside from these findings, our study demonstrates that ciliated cell hypoplasia – with decreased *FOXJ1* and *DNAI1* gene expression – also persists in long-term ALI cultures from COPD patients. In addition, it shows that goblet cell hyperplasia persists in smokers, as witnessed by *SPDEF* upregulation which remains higher in active smokers and ex-smokers that quitted for less than 4 years, as compared with ex-smokers that quitted for more than 4 years (Figures 3F and S2E). These results corroborate previous findings indicating that this secretory trait relates more directly to smoking rather than to the disease (25).

In contrast with those changes, some abnormalities are only observed in short-term culture, such as EMT. EMT is a dynamic process where cells lose their epithelial features and gain mesenchymal properties, including migratory abilities, which is required for normal

embryogenesis (type I EMT), tissue repair (type II), or cancer metastasis (type III). In COPD, airway fibrosis probably follows persistent type II EMT (53). It has been reported that ALI-AE from COPD patients spontaneously exhibit mesenchymal features and that cigarette smoke may induce EMT in control HBEC (7), possibly as a result of TGF-β signalling (19). Accordingly, our results show overexpressed EMT features (vimentin expression, fibronectin release) in the AE from control smokers and COPD patients during the first weeks of culture. However, these features further vanish from weeks 3-4 onwards, with complete disappearance occurring earlier in smoker controls (around week 4) than in COPD (around week 8-10). Moreover, we highlight that, even though EMT markers are vanishing, the COPD AE remains prone to reactivate EMT programming upon inflammatory condition, suggesting the existence of a priming state in the COPD AE, imprinted by previous (*in vivo*) exposures that condition its responses to further stimulation. As observed for EMT, upregulation of IL-8/CXCL-8 release by the smokers' and COPD AE is also fading away from week 7 onwards. In contrast, IL-6 overproduction persisted up to 10 weeks in both smokers' and COPD AE. Finally, *in vitro* exposure to inflammatory cytokines reproduced or aggravated alterations in barrier and polarity features as well as EMT in controls' and COPD AE, respectively.

The fundamental mechanisms of these observations question the nature of epithelial memory. Inflammatory memory refers to memories of previous immune events enabling barrier tissues to rapidly recall distinct environmental exposures, which may be stored not only in immune cells but also in epithelial and mesenchymal cells (31). It was proposed that the memory distribution could promote maladaptation in disease particularly if cellular cooperation is potentiated (i.e. collective memory owing to different cell types) during recall responses. Progenitor basal cells are prime candidate to retain epithelial memory in the airways, as do epithelial progenitors in the skin towards mechanical stress (54) or in the gut towards dietary components (55). Interestingly, it was recently shown that WNT signalling that is involved in

447 the later form of epithelial memory and may regulate stemness and tumorigenicity, is
448 upregulated in the COPD AE (47). In line with the recent hypothesis that basal cells serve as
449 repositories of allergic inflammatory memory in respiratory epithelial cells (31), one could
450 propose that airway basal cells also store the memory of repeated injuries by previous exposures
451 to toxics.

452 Our study has limitations. First, an effect of treatments (especially inhaled corticosteroids in
453 severe patients) on the findings cannot be excluded. However, *in vitro* studies on intestinal cell
454 lines and primary human bronchial and nasal epithelial cells in ALI-culture showed
455 dexamethasone-induced increases in TEER, claudin-2 (56), and E-cadherin (57, 58) expression,
456 while budesonide exposure of ALI-HBEC counter-acted CS-induced barrier dysfunction (59).
457 In addition, dexamethasone and fluticasone propionate improved TGF-β_1-induced EMT in
458 A549 cells and in primary airway nasal cells (60), suggesting that corticosteroids may rather
459 improve barrier function and EMT changes. Second, the imprinting observed in this model of
460 *ex vivo* reconstituted epithelium, that involves (following differentiation of basal cells to a
461 pseudostratified epithelium) long-term culture of non-dividing cells, should be confirmed in
462 other models such as organoids and culture following multiple passages.

463 In conclusion, this study demonstrates that the AE from smokers and COPD stores the memory
464 of its native state and previous insults from cigarette smoking, as well as additional signals that
465 underlie the disease itself. This memory is multidimensional, including alterations in barrier
466 function, epithelial polarity, and lineage differentiation, as well as IL-6 release and propensity
467 to EMT reprogramming. In line with other studies, we suggest that the COPD AE memory is
468 imprinted in progenitor basal cells, which contribute to the persistence of disease by serving as
469 repositories for toxic inflammatory memories in the airways.

References

1. Organization WH. Chronic respiratory diseases. 2017 [Available from: http://www.who.int/respiratory/copd/burden/en/.
2. Salvi SS, Barnes PJ. Chronic obstructive pulmonary disease in non-smokers. Lancet. 2009;374(9691):733-43.
3. Vogelmeier CF, Criner GJ, Martinez FJ, Anzueto A, Barnes PJ, Bourbeau J, et al. Global Strategy for the Diagnosis, Management, and Prevention of Chronic Obstructive Lung Disease 2017 Report. GOLD Executive Summary. Am J Respir Crit Care Med. 2017;195(5):557-82.
4. Celli BR, Anderson JA, Cowans NJ, Crim C, Hartley BF, Martinez FJ, et al. Pharmacotherapy and Lung Function Decline in Patients with Chronic Obstructive Pulmonary Disease: A Systematic Review. Am J Respir Crit Care Med. 2020.
5. Aghapour M, Raee P, Moghaddam SJ, Hiemstra PS, Heijink IH. Airway Epithelial Barrier Dysfunction in Chronic Obstructive Pulmonary Disease: Role of Cigarette Smoke Exposure. Am J Respir Cell Mol Biol. 2018;58(2):157-69.
6. Schamberger AC, Mise N, Jia J, Genoyer E, Yildirim AO, Meiners S, et al. Cigarette smoke-induced disruption of bronchial epithelial tight junctions is prevented by transforming growth factor-beta. Am J Respir Cell Mol Biol. 2014;50(6):1040-52.
7. Milara J, Peiro T, Serrano A, Cortijo J. Epithelial to mesenchymal transition is increased in patients with COPD and induced by cigarette smoke. Thorax. 2013;68(5):410-20.
8. Amatngalim GD, Hiemstra PS. Airway Epithelial Cell Function and Respiratory Host Defense in Chronic Obstructive Pulmonary Disease. Chin Med J (Engl). 2018;131(9):1099-107.
9. Barnes PJ. Cellular and molecular mechanisms of chronic obstructive pulmonary disease. Clin Chest Med. 2014;35(1):71-86.
10. Ghosh M, Miller YE, Nakachi I, Kwon JB, Baron AE, Brantley AE, et al. Exhaustion of Airway Basal Progenitor Cells in Early and Established Chronic Obstructive Pulmonary Disease. Am J Respir Crit Care Med. 2018;197(7):885-96.
11. Crystal RG. Airway basal cells. The "smoking gun" of chronic obstructive pulmonary disease. Am J Respir Crit Care Med. 2014;190(12):1355-62.
12. Yaghi A, Dolovich MB. Airway Epithelial Cell Cilia and Obstructive Lung Disease. Cells. 2016;5(4).
13. Pilette C, Godding V, Kiss R, Delos M, Verbeken E, Decaestecker C, et al. Reduced epithelial expression of secretory component in small airways correlates with airflow obstruction in chronic obstructive pulmonary disease. Am J Respir Crit Care Med. 2001;163(1):185-94.
14. Gamez AS, Gras D, Petit A, Knabe L, Molinari N, Vachier I, et al. Supplementing defect in club cell secretory protein attenuates airway inflammation in COPD. Chest. 2015;147(6):1467-76.
15. Saetta M, Turato G, Baraldo S, Zanin A, Braccioni F, Mapp CE, et al. Goblet cell hyperplasia and epithelial inflammation in peripheral airways of smokers with both symptoms of chronic bronchitis and chronic airflow limitation. Am J Respir Crit Care Med. 2000;161(3 Pt 1):1016-21.

16. Mahmood MQ, Sohal SS, Shukla SD, Ward C, Hardikar A, Noor WD, et al. Epithelial mesenchymal transition in smokers: large versus small airways and relation to airflow obstruction. Int J Chron Obstruct Pulmon Dis. 2015;10:1515-24.

17. Sohal SS. Chronic Obstructive Pulmonary Disease (COPD) and Lung Cancer: Epithelial Mesenchymal Transition (EMT), the Missing Link? EBioMedicine. 2015;2(11):1578-9.

18. Gohy S, Carlier FM, Fregimilicka C, Detry B, Lecocq M, Ladjemi MZ, et al. Altered generation of ciliated cells in chronic obstructive pulmonary disease. Sci Rep. 2019;9(1):17963.

19. Gohy ST, Hupin C, Fregimilicka C, Detry BR, Bouzin C, Gaide Chevronay H, et al. Imprinting of the COPD airway epithelium for dedifferentiation and mesenchymal transition. Eur Respir J. 2015;45(5):1258-72.

20. Barnes PJ. Inflammatory mechanisms in patients with chronic obstructive pulmonary disease. J Allergy Clin Immunol. 2016;138(1):16-27.

21. Eapen MS, Myers S, Walters EH, Sohal SS. Airway inflammation in chronic obstructive pulmonary disease (COPD): a true paradox. Expert Rev Respir Med. 2017;11(10):827-39.

22. Keatings VM, Collins PD, Scott DM, Barnes PJ. Differences in interleukin-8 and tumor necrosis factor-alpha in induced sputum from patients with chronic obstructive pulmonary disease or asthma. Am J Respir Crit Care Med. 1996;153(2):530-4.

23. Rutgers SR, Timens W, Kaufmann HF, van der Mark TW, Koeter GH, Postma DS. Comparison of induced sputum with bronchial wash, bronchoalveolar lavage and bronchial biopsies in COPD. Eur Respir J. 2000;15(1):109-15.

24. Di Stefano A, Capelli A, Lusuardi M, Balbo P, Vecchio C, Maestrelli P, et al. Severity of airflow limitation is associated with severity of airway inflammation in smokers. Am J Respir Crit Care Med. 1998;158(4):1277-85.

25. Lapperre TS, Sont JK, van Schadewijk A, Gosman MM, Postma DS, Bajema IM, et al. Smoking cessation and bronchial epithelial remodelling in COPD: a cross-sectional study. Respir Res. 2007;8:85.

26. Willemse BW, Postma DS, Timens W, ten Hacken NH. The impact of smoking cessation on respiratory symptoms, lung function, airway hyperresponsiveness and inflammation. Eur Respir J. 2004;23(3):464-76.

27. Bai JW, Chen XX, Liu S, Yu L, Xu JF. Smoking cessation affects the natural history of COPD. Int J Chron Obstruct Pulmon Dis. 2017;12:3323-8.

28. Louhelainen N, Rytila P, Haahtela T, Kinnula VL, Djukanovic R. Persistence of oxidant and protease burden in the airways after smoking cessation. BMC Pulm Med. 2009;9:25.

29. Gamble E, Grootendorst DC, Hattotuwa K, O'Shaughnessy T, Ram FS, Qiu Y, et al. Airway mucosal inflammation in COPD is similar in smokers and ex-smokers: a pooled analysis. Eur Respir J. 2007;30(3):467-71.

30. Lapperre TS, Postma DS, Gosman MM, Snoeck-Stroband JB, ten Hacken NH, Hiemstra PS, et al. Relation between duration of smoking cessation and bronchial inflammation in COPD. Thorax. 2006;61(2):115-21.

31. Ordovas-Montanes J, Beyaz S, Rakoff-Nahoum S, Shalek AK. Distribution and storage of inflammatory memory in barrier tissues. Nat Rev Immunol. 2020;20(5):308-20.

32. Bustin SA, Benes V, Garson J, Hellemans J, Huggett J, Kubista M, et al. The need for transparency and good practices in the qPCR literature. Nat Methods. 2013;10(11):1063-7.

546 33. Pilette C, Ouadrhiri Y, Dimanche F, Vaerman JP, Sibille Y. Secretory component is cleaved by neutrophil
547 serine proteinases but its epithelial production is increased by neutrophils through NF-kappa B- and p38 mitogen-
548 activated protein kinase-dependent mechanisms. Am J Respir Cell Mol Biol. 2003;28(4):485-98.
549 34. Collin AM, Lecocq M, Noel S, Detry B, Carlier FM, Aboubakar Nana F, et al. Lung immunoglobulin A
550 immunity dysregulation in cystic fibrosis. EBioMedicine. 2020;60:102974.
551 35. Kim V, Oros M, Durra H, Kelsen S, Aksoy M, Cornwell WD, et al. Chronic bronchitis and current
552 smoking are associated with more goblet cells in moderate to severe COPD and smokers without airflow
553 obstruction. PLoS One. 2015;10(2):e0116108.
554 36. Chen G, Korfhagen TR, Karp CL, Impey S, Xu Y, Randell SH, et al. Foxa3 induces goblet cell metaplasia
555 and inhibits innate antiviral immunity. Am J Respir Crit Care Med. 2014;189(3):301-13.
556 37. Park KS, Korfhagen TR, Bruno MD, Kitzmiller JA, Wan H, Wert SE, et al. SPDEF regulates goblet cell
557 hyperplasia in the airway epithelium. J Clin Invest. 2007;117(4):978-88.
558 38. Rajavelu P, Chen G, Xu Y, Kitzmiller JA, Korfhagen TR, Whitsett JA. Airway epithelial SPDEF
559 integrates goblet cell differentiation and pulmonary Th2 inflammation. J Clin Invest. 2015;125(5):2021-31.
560 39. Di Stefano A, Capelli A, Donner CF. Role of interleukin-8 in the pathogenesis and treatment of COPD.
561 Chest. 2004;126(3):676-8.
562 40. Barnes PJ, Burney PG, Silverman EK, Celli BR, Vestbo J, Wedzicha JA, et al. Chronic obstructive
563 pulmonary disease. Nat Rev Dis Primers. 2015;1:15076.
564 41. Bafadhel M, McKenna S, Terry S, Mistry V, Reid C, Haldar P, et al. Acute exacerbations of chronic
565 obstructive pulmonary disease: identification of biologic clusters and their biomarkers. Am J Respir Crit Care
566 Med. 2011;184(6):662-71.
567 42. Anthonisen NR, Connett JE, Kiley JP, Altose MD, Bailey WC, Buist AS, et al. Effects of smoking
568 intervention and the use of an inhaled anticholinergic bronchodilator on the rate of decline of FEV1. The Lung
569 Health Study. JAMA. 1994;272(19):1497-505.
570 43. Fletcher C, Peto R. The natural history of chronic airflow obstruction. Br Med J. 1977;1(6077):1645-8.
571 44. Ramos EM, De Toledo AC, Xavier RF, Fosco LC, Vieira RP, Ramos D, et al. Reversibility of impaired
572 nasal mucociliary clearance in smokers following a smoking cessation programme. Respirology. 2011;16(5):849-
573 55.
574 45. Verra F, Escudier E, Lebargy F, Bernaudin JF, De Cremoux H, Bignon J. Ciliary abnormalities in
575 bronchial epithelium of smokers, ex-smokers, and nonsmokers. Am J Respir Crit Care Med. 1995;151(3 Pt 1):630-
576 4.
577 46. Willemse BW, ten Hacken NH, Rutgers B, Lesman-Leegte IG, Postma DS, Timens W. Effect of 1-year
578 smoking cessation on airway inflammation in COPD and asymptomatic smokers. Eur Respir J. 2005;26(5):835-
579 45.
580 47. Carlier FM, Dupasquier S, Ambroise J, Detry B, Lecocq M, Bietry-Claudet C, et al. Canonical WNT
581 pathway is activated in the airway epithelium in chronic obstructive pulmonary disease. EBioMedicine.
582 2020;61:103034.
583 48. Gohy ST, Detry BR, Lecocq M, Bouzin C, Weynand BA, Amatngalim GD, et al. Polymeric
584 immunoglobulin receptor down-regulation in chronic obstructive pulmonary disease. Persistence in the cultured
585 epithelium and role of transforming growth factor-beta. Am J Respir Crit Care Med. 2014;190(5):509-21.

586 49. Carlier F, Detry B, Sibille Y, Pilette C. COPD epithelial phenotype shows partial reversibility in long-
587 term primary epithelial ALI-cultures. Eur Respir J. 2018;52(suppl 62).
588 50. Shaykhiev R, Otaki F, Bonsu P, Dang DT, Teater M, Strulovici-Barel Y, et al. Cigarette smoking
589 reprograms apical junctional complex molecular architecture in the human airway epithelium in vivo. Cell Mol
590 Life Sci. 2011;68(5):877-92.
591 51. Cereijido M, Valdes J, Shoshani L, Contreras RG. Role of tight junctions in establishing and maintaining
592 cell polarity. Annu Rev Physiol. 1998;60:161-77.
593 52. Ladjemi MZ, Gras D, Dupasquier S, Detry B, Lecocq M, Garulli C, et al. Bronchial Epithelial IgA
594 Secretion Is Impaired in Asthma. Role of IL-4/IL-13. Am J Respir Crit Care Med. 2018;197(11):1396-409.
595 53. Bartis D, Mise N, Mahida RY, Eickelberg O, Thickett DR. Epithelial-mesenchymal transition in lung
596 development and disease: does it exist and is it important? Thorax. 2014;69(8):760-5.
597 54. Naik S, Larsen SB, Gomez NC, Alaverdyan K, Sendoel A, Yuan S, et al. Inflammatory memory sensitizes
598 skin epithelial stem cells to tissue damage. Nature. 2017;550(7677):475-80.
599 55. Beyaz S, Mana MD, Roper J, Kedrin D, Saadatpour A, Hong SJ, et al. High-fat diet enhances stemness
600 and tumorigenicity of intestinal progenitors. Nature. 2016;531(7592):53-8.
601 56. Fischer A, Gluth M, Weege F, Pape UF, Wiedenmann B, Baumgart DC, et al. Glucocorticoids regulate
602 barrier function and claudin expression in intestinal epithelial cells via MKP-1. Am J Physiol Gastrointest Liver
603 Physiol. 2014;306(3):G218-28.
604 57. Carayol N, Vachier I, Campbell A, Crampette L, Bousquet J, Godard P, et al. Regulation of E-cadherin
605 expression by dexamethasone and tumour necrosis factor-alpha in nasal epithelium. Eur Respir J.
606 2002;20(6):1430-6.
607 58. Carayol N, Campbell A, Vachier I, Mainprice B, Bousquet J, Godard P, et al. Modulation of cadherin and
608 catenins expression by tumor necrosis factor-alpha and dexamethasone in human bronchial epithelial cells. Am J
609 Respir Cell Mol Biol. 2002;26(3):341-7.
610 59. Heijink I, van den Berge M, Kliphuis N, ten Hacken N, Postma D, van Oosterhout A. Corticosteroids
611 improve airway epithelial regeneration and restore oxidative stress-induced epithelial barrier dysfunction. Eur
612 Respir J. 2012;40(Suppl 56).
613 60. Yang HW, Lee SA, Shin JM, Park IH, Lee HM. Glucocorticoids ameliorate TGF-beta1-mediated
614 epithelial-to-mesenchymal transition of airway epithelium through MAPK and Snail/Slug signaling pathways. Sci
615 Rep. 2017;7(1):3486.

616

Tables

	Non-smoker controls (n=10)	Smoker controls (n=15)	COPD 1-2 (n=13)	COPD 3-4 (n=13)	
N (Male/Female)	10 (4/6)	15 (11/4)	13 (6/7)	13 (5/8)	ns
Age (y)	68.7 ± 13.2	64.2 ± 9.0	64.4 ± 9.5	59.8 ± 4.6	ns
Smoking history (never/former/current n)	10/0/0	0/10/5	0/4/9	0/13/0	p=0.001
Pack-years	0.0 ± 0	32.5 ± 20.7*	43.1 ± 19.6*	43.2 ± 23.1*	p<0.0001
If applicable, duration since smoking cessation (mo)	NA	154.0 ± 154.1	50.0 ± 55.5	90.6 ± 87.0	ns
FEV1 (% of PV)	104.8 ± 15.5	95.5 ± 14.7	74.1 ± 9.7*#	23.6 ± 6.1*#¶	p<0.0001
FEV1/VC ratio (%)	79.4 ± 6.9	78.5 ± 6.8	59.9 ± 9.3*#	45.3 ± 17.0*#¶	p<0.0001
DLCO (% of PV)	77.7 ± 13.0	69.9 ± 14.1	59.2 ± 19.1*	35.6 ± 8.0*#¶	p<0.0001
BMI ($kg.m^{-2}$)	27.8 ± 5.7	26.7 ± 5.2	25.4 ± 5.8	23.8 ± 4.0	ns
Inhaled corticosteroids (n/total N)	0/10	1/15	1/13	12/13	p<0.0001

Table 1 | Patient cohort for ALI-cultures. Data are presented as mean ± SD, unless otherwise stated. Demographic data, lung function tests, smoking history and inhaled corticotherapy are stated for the patient groups, classified according to smoking history and the presence and severity of airflow limitation. ALI, air/liquid interface; BMI, body mass index; COPD, chronic obstructive pulmonary disease; DLCO, diffusing capacity of the lung for CO; FEV1, forced expiratory volume in 1 s; mo, months; PV, predicted values; SD, standard deviation; VC, vital capacity; y, years.
* = p<0.05 compared to non-smoker controls
# = p<0.05 compared to smoker controls
¶ = p<0.05 compared to COPD stage 1-2 patients
ns, not significant

Figures legends

Figure 1 | COPD and smokers AE displays persistent decreased TEER compared with non-smokers AE.

A-D. TEER in the ALI-AE from non-smokers and smoker controls and COPD patients (GOLD classification from 1 to 4 according to the spirometric severity of the disease). Severe and very severe COPD AE show a sharp decrease in TEER as compared with (non)-smokers at all time periods (1 to 8 weeks), that is also observed to a lesser extent in mild and moderate COPD

E-G. The barrier dysfunction observed in COPD, witnessed by the TEER decrease, significantly correlates with the disease severity assessed by the FEV1. This is observed from 2 weeks ALI (**E**) up to 8 weeks (**G**).

H. Longitudinal analysis of the evolution of the TEER in the ALI-AE from non-smokers, smoker controls, mild-to-moderate COPD and (very) severe COPD patients, showing a smoking-related persistent barrier dysfunction that is further enhanced in COPD. °, $^{\#}$, §, $^{£}$, < 0.0001, $^{\$}$, ¶ < 0.001, mixed model analysis.

*, **, ***, **** indicate p-values of less than 0.05, 0.01, 0.001, and 0.0001, respectively (analysed using the Kruskal-Wallis test followed by Dunn's post-hoc test, except for H). Bars indicate median ± interquartile range, except for H, mean ± SEM. °: CT NS *versus* Smo; $^{\#}$: CT NS *versus* COPD 1-2, §: CT NS *versus* COPD 3-4, $^{\$}$: CT S *versus* COPD 1-2, $^{£}$: CT S *versus* COPD 3-4, ¶: COPD 1-2 *versus* COPD 3-4

AE, airway epithelium; ALI, air-liquid interface; COPD, chronic obstructive pulmonary disease; FEV1, forced expired volume in 1 second; GAPDH, glyceralderhyde-3-phosphate dehydrogenase; NS, non-smokers; SEM, standard error of the mean; Smo, smokers; TEER, transepithelial electric resistance; w, weeks.

Figure 2 | COPD and smokers AE displays decreased E-cadherin and occludin protein expression compared with non-smokers AE.

A-D. Decreased E-cadherin protein levels at 1 and 3 weeks, but no more at 6 and 9 weeks, in smoker controls and COPD ALI-AE as compared with that of non-smokers.

E-G. Decreased occludin protein levels, observable from 3 weeks up to 9 weeks, in smoker controls and COPD ALI-AE as compared with that of non-smokers.

H. Occludin decrease in COPD AE significantly correlates with disease severity witnessed by the FEV1.

I. Representative blots for E-cadherin in non-smokers and very severe COPD AE, at 1 and 3 weeks, showing decreased expression of E-cadherin at these time periods in COPD.

J. Representative blots for occludin in non-smokers and very severe COPD AE, at 6 and 9 weeks, showing decreased expression of occludin at these time periods in COPD.

*, **, *** indicate p-values of less than 0.05, 0.01, and 0.001, respectively (analysed using the Kruskal-Wallis test followed by Dunn's post-hoc test). Bars indicate median ± interquartile range.

AE, airway epithelium; ALI, air-liquid interface; COPD, chronic obstructive pulmonary disease; FEV1, forced expired volume in 1 second; NS, non-smokers; ns, not significant; SEM, standard error of the mean; Smo, smokers; w, weeks.

Figure 3 | Altered differentiation programming in smoker controls and COPD patients.

A. Decreased *MYB* expression in smokers and COPD AE, at 1, 2, and 8 weeks ALI culture. Longitudinal analysis shows a strong, persistent down expression as compared with non-smokers. Right graph: $^{\#}$, $^{\S} < 0.0001$, $^{\circ} < 0.001$, $^{£} = 0.07$, mixed model analysis.

B. Decreased *FOXJ1* expression in smokers and COPD AE, at 1, 2, and 8 weeks ALI culture. Longitudinal analysis shows a strong, persistent down expression as compared with non-smokers. Right graph: $^{\#}$, $^{\S} < 0.0001$, $^{\circ} < 0.001$, mixed model analysis.

C. Decreased *DNAI1* expression in smokers and COPD AE, at 2, 4 and 8 weeks ALI culture. Longitudinal analysis shows a strong, persistent down expression as compared with non-smokers. Right graph: $^{\#}$, §, $^{\circ} < 0.0001$, mixed model analysis.

D. *MYB*, *FOXJ1*, and *DNAI1* downregulation in COPD patients correlates moderately with the disease severity, assessed by the FEV1.

E. Increased *SPDEF* expression in smokers AE as compared with non-smokers at 2, 4 and 8 weeks ALI culture. Moreover, complementary longitudinal analysis shows increased expression in smokers as compared with COPD. Right graph: $^{\#}$, $^{\S} < 0.01$, $^{£} < 0.05$, mixed model analysis.

F. SPDEF expression is decreased in smokers who quitted smoking for more than 4 years.

*, **, ***, **** indicate p-values of less than 0.05, 0.01, 0.001, and 0.0001, respectively (analysed using the Kruskal-Wallis test followed by Dunn's post-hoc test, except for longitudinal data, mixed model). Bars indicate median ± interquartile range, except for longitudinal analysis, mean ± SEM. °: CT NS *versus* Smo; $^{\#}$: CT NS *versus* COPD 1-2, §: CT NS *versus* COPD 3-4, $^{£}$: CT S *versus* COPD 3-4.

AE, airway epithelium; ALI, air-liquid interface; COPD, chronic obstructive pulmonary disease; CT, control; FEV1, forced expired volume in 1 second; HKG, housekeeping genes; NS, non-smokers; SEM, standard error of the mean; Smo, smokers; w, weeks.

Figure 4 | COPD-related EMT features fade away after 7 to 10 weeks ALI culture.

A. Increased vimentin expression rapidly (1 week) disappears in smokers but persists up to 5 weeks in (very) severe COPD AE.

B. Illustrative gels from non-smokers and very severe COPD-derived AE at 1, 3 and 5 weeks, illustrating the vimentin increased content in COPD.

C. Increased fibronectin release disappears after 1 week ALI culture in smokers AE, after 4 weeks in mild-to-moderate COPD AE, while it persists up to 7 weeks in (very) severe COPD AE.

D. Longitudinal analysis of the fibronectin release over time. °, $^{\#} < 0.05$; $^{\S} < 0.01$, mixed model analysis.

*, **, *** indicate p-values of less than 0.05, 0.01, and 0.001, respectively (analysed using the Kruskal-Wallis test followed by Dunn's post-hoc test, except for D, mixed model). Bars indicate median ± interquartile range, except for D, mean ± SEM. °: CT NS *versus* Smo; $^{\#}$: CT NS *versus* COPD 1-2, §: CT NS *versus* COPD 3-4.

AE, airway epithelium; ALI, air-liquid interface; COPD, chronic obstructive pulmonary disease; GAPDH, glyceraldehyde-3-phosphate dehydrogenase; NS, non-smokers; ns, not significant; SEM, standard error of the mean; Smo, smokers; w, weeks.

Figure 5 | Impaired polarity, witnessed by a disruption and a delayed acquisition of the PIGR/SC system, is imprinted in the COPD AE.

A. SC apical release in ALI-AE from smokers and COPD patients is decreased as compared with non-smokers, from 2 weeks culture onwards, up to 10 weeks.

B. SC decreased release in the COPD AE moderately correlates with the disease severity, witnessed by the FEV1. Longitudinal analysis of SC apical release demonstrates a decreased release in smokers and mild-to-moderate COPD, as compared with non-smokers. This impaired SC production is enhanced in (very) severe COPD AE. °, $^{\#}$, $^{\S} < 0.0001$; $^{£}$, $^{¶} < 0.001$, mixed model analysis.

C. *PIGR* gene expression is not significantly decreased in (very) severe COPD ALI-AE at separate time-points, as depicted here at 8 weeks (see also Figure S4B), but longitudinal analysis shows a significant decrease in *PIGR* expression in (very) severe COPD AE as

compared with non-smokers, smokers and mild-to-moderate COPD. $^{£}$, ¶ < 0.001, § < 0.01, mixed model analysis.

D. pIgR acquisition is delayed during the differentiation of the AE in COPD as compared with non-smokers, as represented at 2 weeks ALI culture, and catches it up only after 4 weeks.

*, **, ***, **** indicate p-values of less than 0.05, 0.01, 0.001, and 0.0001, respectively (analysed using the Kruskal-Wallis test followed by Dunn's post-hoc test, except for longitudinal analysis in B and C, mixed model). Bars indicate median ± interquartile range, except for longitudinal analysis in B and C, mean ± SEM.

°: CT NS *versus* Smo; $^{#}$: CT NS *versus* COPD 1-2, §: CT NS *versus* COPD 3-4, $^{£}$: CT S *versus* COPD 3-4, ¶: COPD 1-2 *versus* COPD 3-4

AE, airway epithelium; ALI, air-liquid interface; COPD, chronic obstructive pulmonary disease; FEV1, forced expired volume in 1 second; GAPDH, glyceraldehyde-3-phosphate dehydrogenase; HKG, housekeeping genes; NS, non-smokers; ns, not significant; pIgR, polymeric immunoglobulin receptor; PV, predicted values; SC, secretory component; SEM, standard error of the mean; Smo, smokers; w, weeks.

Figure 6 | Epithelial release of inflammatory cytokines partly persists in COPD AE.

A. IL-8/CXCL-8 production by the reconstituted ALI-AE is increased in smokers and COPD at 1, 2 and 4 weeks, but disappears afterwards, although a non-significant upward trend persists. °, $^{#}$, § < 0.0001, mixed model analysis.

B. IL-6 production by the reconstituted ALI-AE is increased in smokers and COPD and persists up to 9 weeks.

*, ** indicate p-values of less than 0.05 and 0.01, respectively (analysed using the Kruskal-Wallis test followed by Dunn's post-hoc test, except for longitudinal analysis, mixed model). Bars indicate median ± interquartile range, except for longitudinal analysis, mean. °, $^{#}$, § < 0.0001, mixed model analysis.

°: CT NS *versus* Smo; $^{#}$: CT NS *versus* COPD 1-2, §: CT NS *versus* COPD 3-4.

AE, airway epithelium; ALI, air-liquid interface; COPD, chronic obstructive pulmonary disease; IL, interleukin; NS, non-smokers; ns, not significant; SEM, standard error of the mean; Smo, smokers; w, weeks.

Figure 7 | Cytokine activation triggers COPD-like epithelial changes.

A. Epithelial inflammation, driven by exogenous TNF-α, IL-1β and IL-6, induces barrier dysfunction, witnessed by a dramatic decrease in TEER that is present in each group (NS, Smo, COPD 1-2, COPD 3-4).

B-D. Cytokine-induced epithelial inflammation induces EMT in smokers and COPD-derived ALI AE, witnessed by increased fibronectin release at 1, 2 and 4 weeks (B) and vimentin expression at 4 weeks (D). The absolute increase in fibronectin and vimentin was significantly higher in COPD AE than in controls (pooled smokers and non-smokers) (C, D).

E. Cytokine-induced epithelial inflammation deteriorates the epithelial polarity, witnessed by the SC apical release. No difference was seen in (very) severe COPD, due to low baseline levels.

*, **, ***, **** indicate p-values of less than 0.05, 0.01, 0.001, and 0.0001, respectively (analysed using the Mann-Whitney test for B, C and D, and a mixed model for A and E). Bars indicate median ± interquartile range for B, C and D, and mean ± SEM for A and E.

AE, airway epithelium; ALI, air-liquid interface; COPD, chronic obstructive pulmonary disease; CT, controls; EMT, epithelial-to-mesenchymal transition; GAPDH, glyceraldehyde-3-phosphate dehydrogenase; IL, interleukin; NS, non-smokers; ns, not significant; SC, secretory component; SEM, standard error of the mean; Smo, smokers; TEER, transepithelial electric resistance; TNF-α, tumour necrosis factor α; w, weeks.

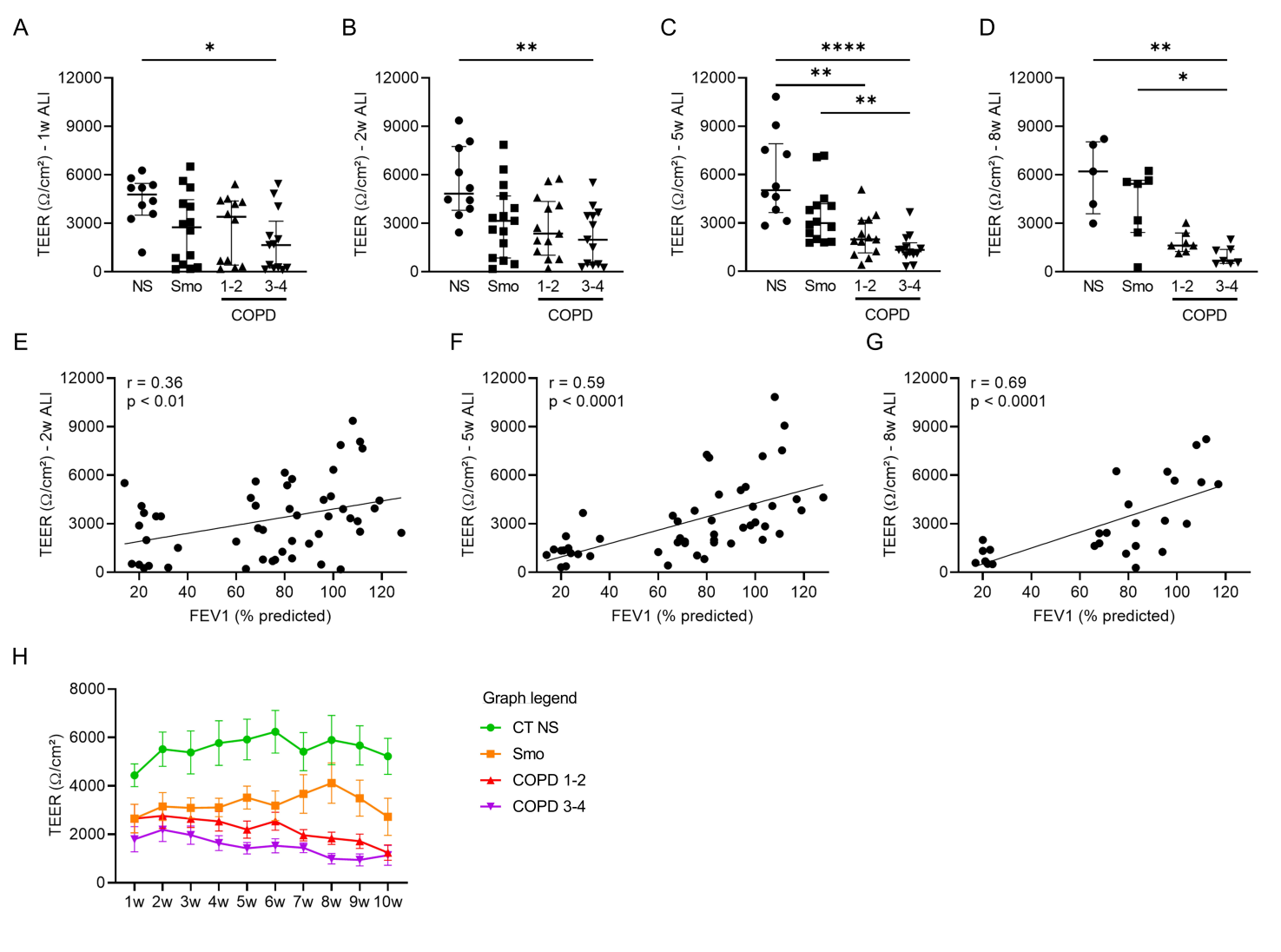
A
B
C
D
TEER (Ω/cm²) - 1w ALI
TEER (Ω/cm²) - 2w ALI
TEER (Ω/cm²) - 5w ALI
TEER (Ω/cm²) - 8w ALI
12000
9000
6000
3000
0
NS
Smo
1-2
3-4
COPD
*
**
****
E
F
G
r = 0.36
p < 0.01
r = 0.59
p < 0.0001
r = 0.69
p < 0.0001
FEV1 (% predicted)
20
40
60
80
100
120
H
TEER (Ω/cm²)
8000
6000
4000
2000
0
1w
2w
3w
4w
5w
6w
7w
8w
9w
10w
Graph legend
CT NS
Smo
COPD 1-2
COPD 3-4

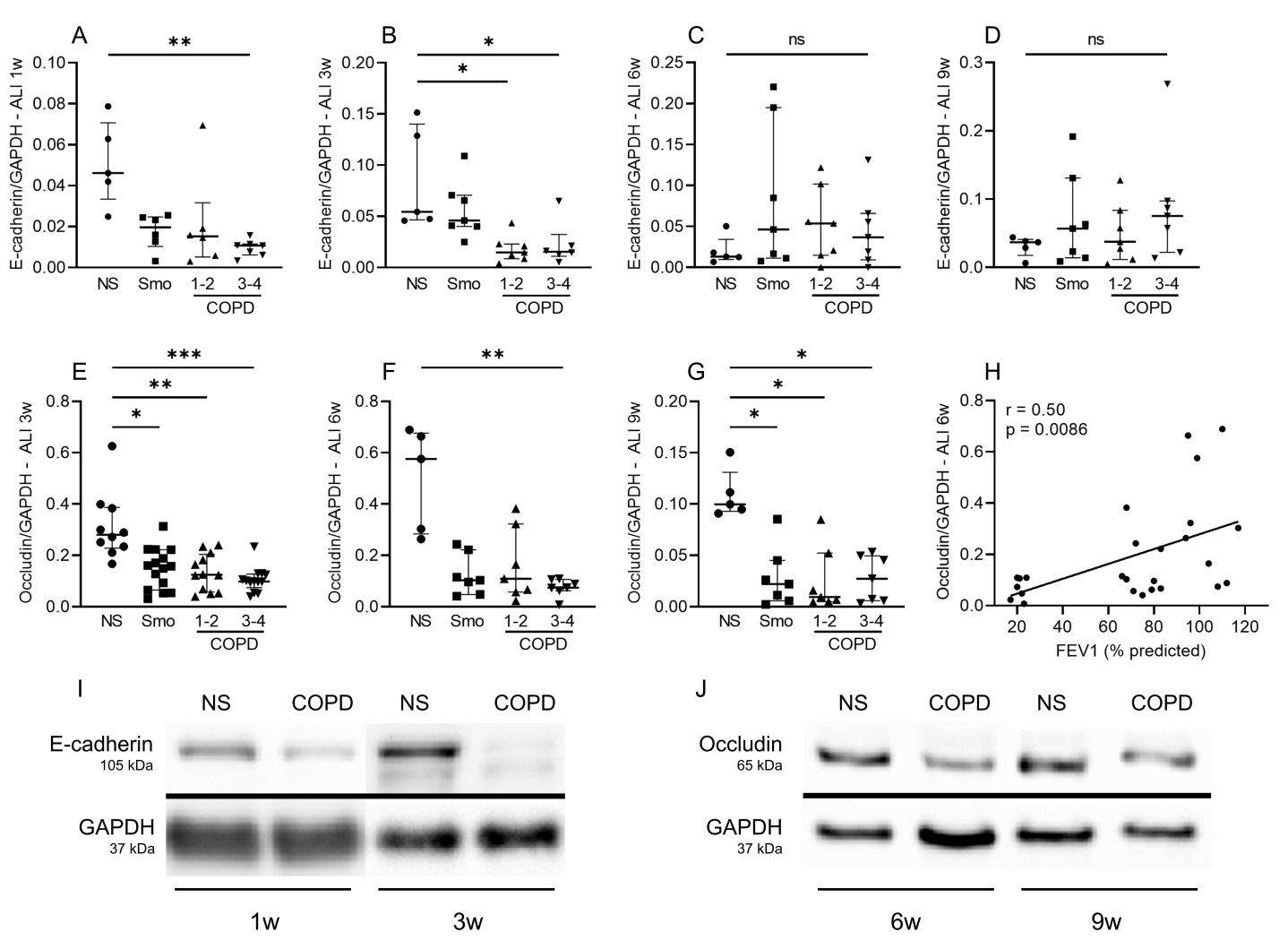
A
B
C
D
E
F
G
H
I
J
E-cadherin/GAPDH - ALI 1w
E-cadherin/GAPDH - ALI 3w
E-cadherin/GAPDH - ALI 6w
E-cadherin/GAPDH - ALI 9w
Occludin/GAPDH - ALI 3w
Occludin/GAPDH - ALI 6w
Occludin/GAPDH - ALI 9w
NS
Smo
1-2
3-4
COPD
ns
r = 0.50
p = 0.0086
FEV1 (% predicted)
E-cadherin
105 kDa
Occludin
65 kDa
GAPDH
37 kDa
1w
3w
6w
9w

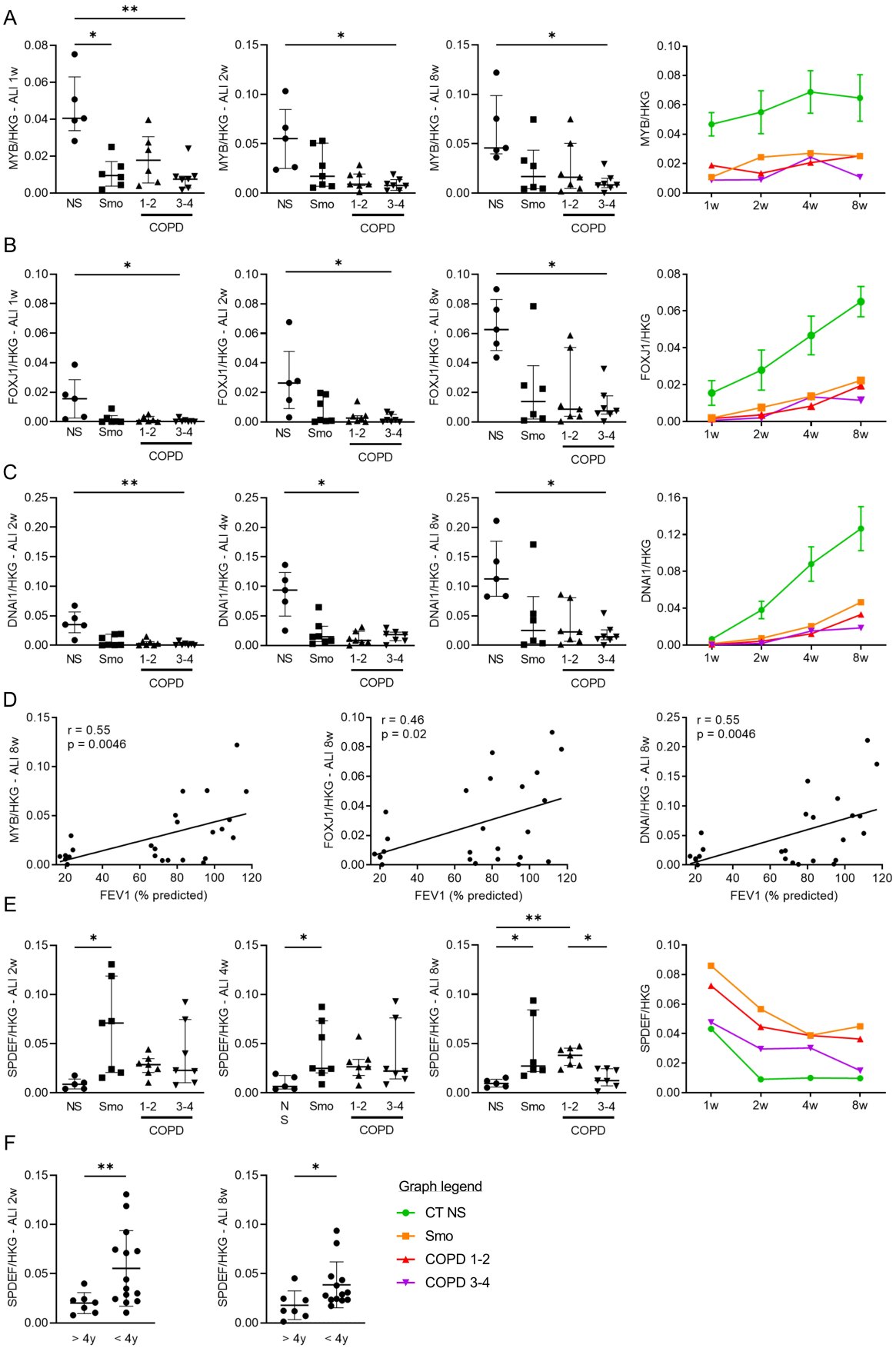
A
MYB/HKG - ALI 1w
MYB/HKG - ALI 2w
MYB/HKG - ALI 8w
MYB/HKG
B
FOXJ1/HKG - ALI 1w
FOXJ1/HKG - ALI 2w
FOXJ1/HKG - ALI 8w
FOXJ1/HKG
C
DNAI1/HKG - ALI 2w
DNAI1/HKG - ALI 4w
DNAI1/HKG - ALI 8w
DNAI1/HKG
D
MYB/HKG - ALI 8w
r = 0.55
p = 0.0046
FEV1 (% predicted)
FOXJ1/HKG - ALI 8w
r = 0.46
p = 0.02
DNAI/HKG - ALI 8w
r = 0.55
p = 0.0046
E
SPDEF/HKG - ALI 2w
SPDEF/HKG - ALI 4w
SPDEF/HKG - ALI 8w
SPDEF/HKG
F
SPDEF/HKG - ALI 2w
SPDEF/HKG - ALI 8w
> 4y
< 4y
Graph legend
CT NS
Smo
COPD 1-2
COPD 3-4
NS
Smo
1-2
3-4
COPD
1w
2w
4w
8w

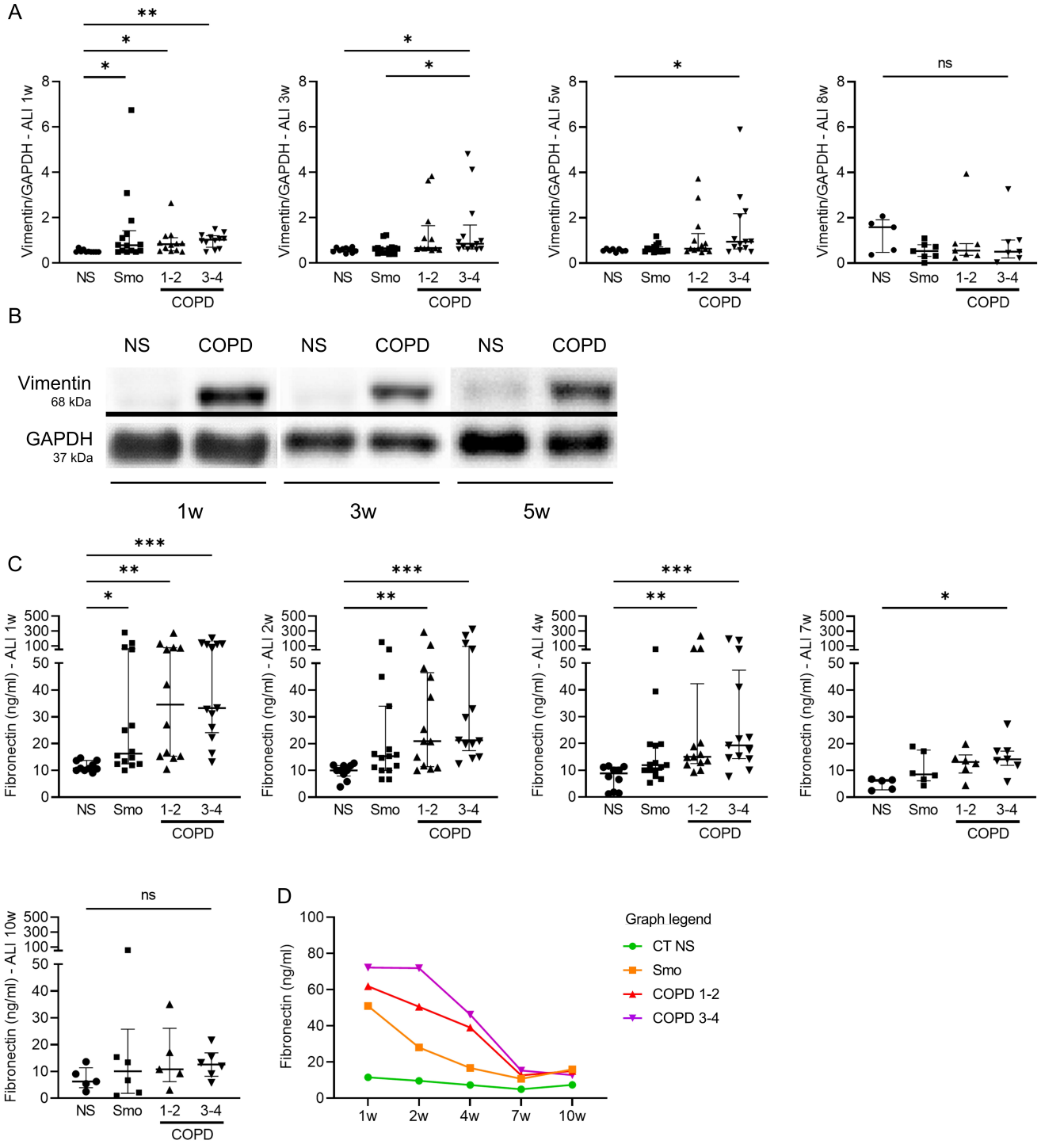
A
Vimentin/GAPDH - ALI 1w
Vimentin/GAPDH - ALI 3w
Vimentin/GAPDH - ALI 5w
Vimentin/GAPDH - ALI 8w
NS
Smo
1-2
3-4
COPD
ns
B
NS
COPD
Vimentin
68 kDa
GAPDH
37 kDa
1w
3w
5w
C
Fibronectin (ng/ml) - ALI 1w
Fibronectin (ng/ml) - ALI 2w
Fibronectin (ng/ml) - ALI 4w
Fibronectin (ng/ml) - ALI 7w
Fibronectin (ng/ml) - ALI 10w
D
Fibronectin (ng/ml)
Graph legend
CT NS
Smo
COPD 1-2
COPD 3-4
1w
2w
4w
7w
10w

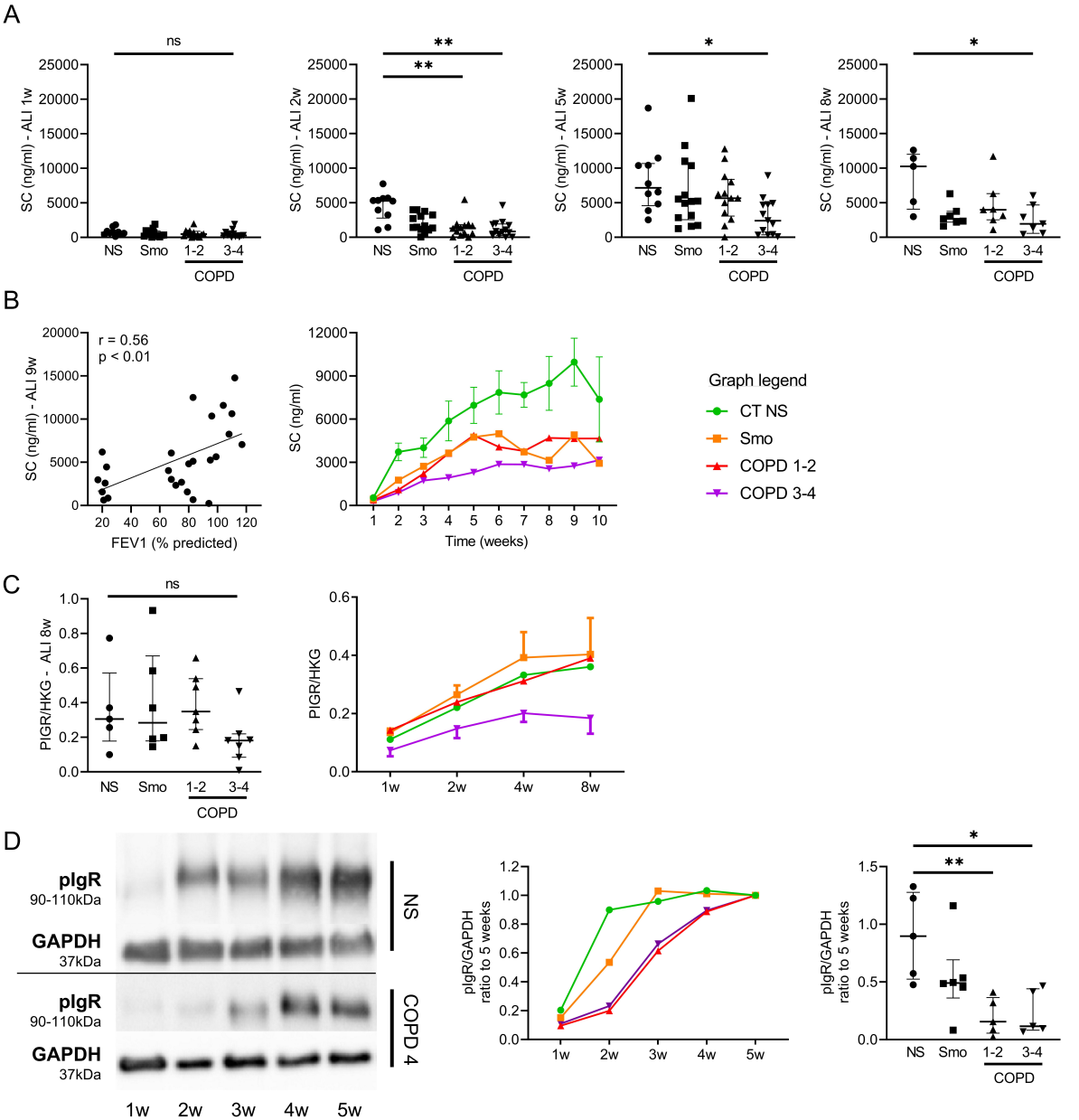
A
ns
**
**
*
*
SC (ng/ml) - ALI 1w
SC (ng/ml) - ALI 2w
SC (ng/ml) - ALI 5w
SC (ng/ml) - ALI 8w
25000
20000
15000
10000
5000
0
NS
Smo
1-2
3-4
COPD
B
r = 0.56
p < 0.01
SC (ng/ml) - ALI 9w
FEV1 (% predicted)
20
40
60
80
100
120
SC (ng/ml)
Time (weeks)
12000
9000
6000
3000
1
2
3
4
5
6
7
8
9
10
Graph legend
CT NS
Smo
COPD 1-2
COPD 3-4
C
ns
PIGR/HKG - ALI 8w
PIGR/HKG
1.0
0.8
0.6
0.4
0.2
0.0
1w
2w
4w
8w
D
pIgR
90-110kDa
GAPDH
37kDa
NS
COPD 4
1w
2w
3w
4w
5w
pIgR/GAPDH
ratio to 5 weeks
1.2
1.0
0.8
0.6
0.4
0.2
0.0
*
**
1.5
1.0
0.5

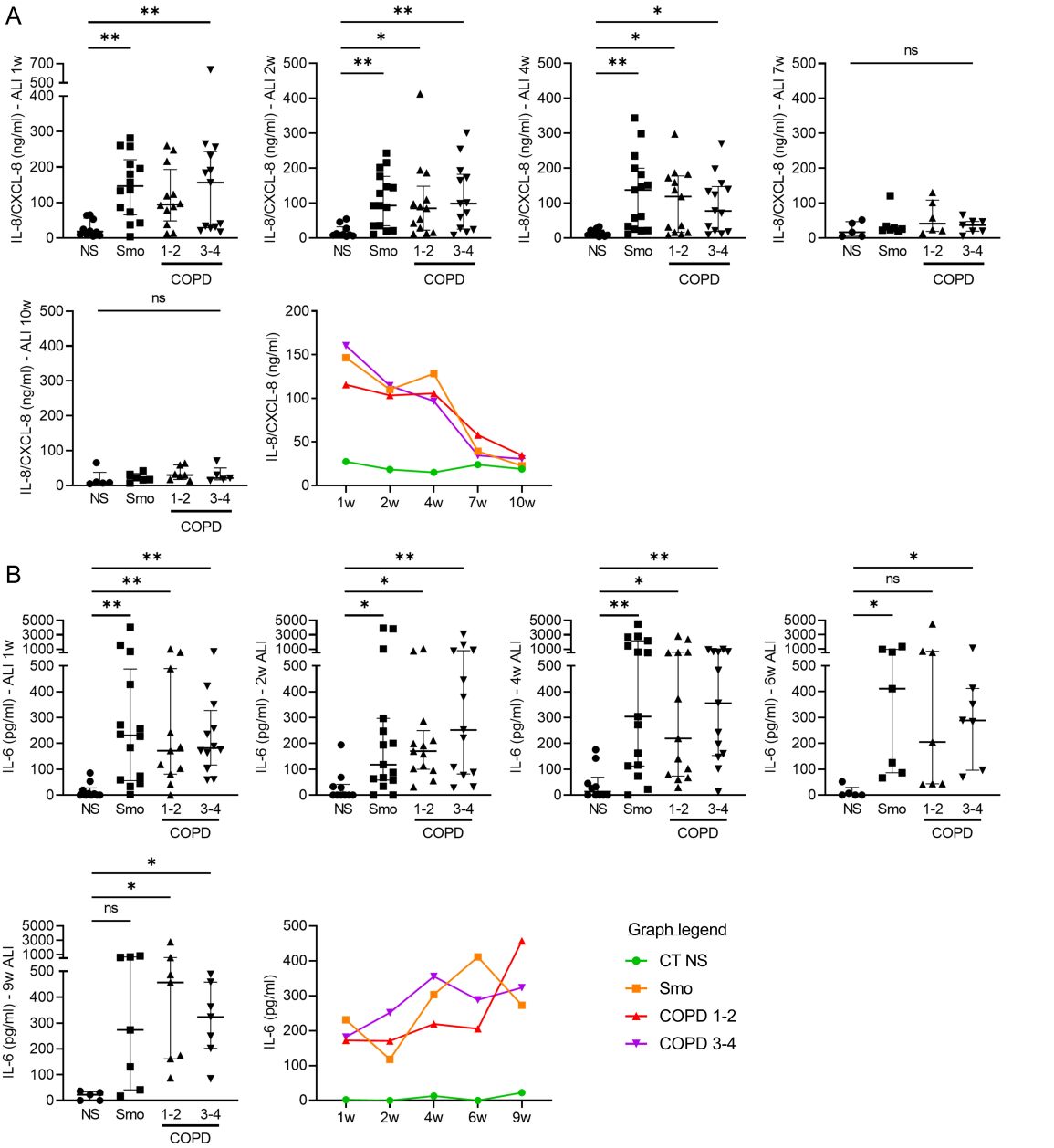
A
IL-8/CXCL-8 (ng/ml) - ALI 1w
IL-8/CXCL-8 (ng/ml) - ALI 2w
IL-8/CXCL-8 (ng/ml) - ALI 4w
IL-8/CXCL-8 (ng/ml) - ALI 7w
IL-8/CXCL-8 (ng/ml) - ALI 10w
IL-8/CXCL-8 (ng/ml)
NS
Smo
1-2
3-4
COPD
ns
1w
2w
4w
7w
10w
B
IL-6 (pg/ml) - ALI 1w
IL-6 (pg/ml) - 2w ALI
IL-6 (pg/ml) - 4w ALI
IL-6 (pg/ml) - 6w ALI
IL-6 (pg/ml) - 9w ALI
IL-6 (pg/ml)
6w
9w
Graph legend
CT NS
Smo
COPD 1-2
COPD 3-4

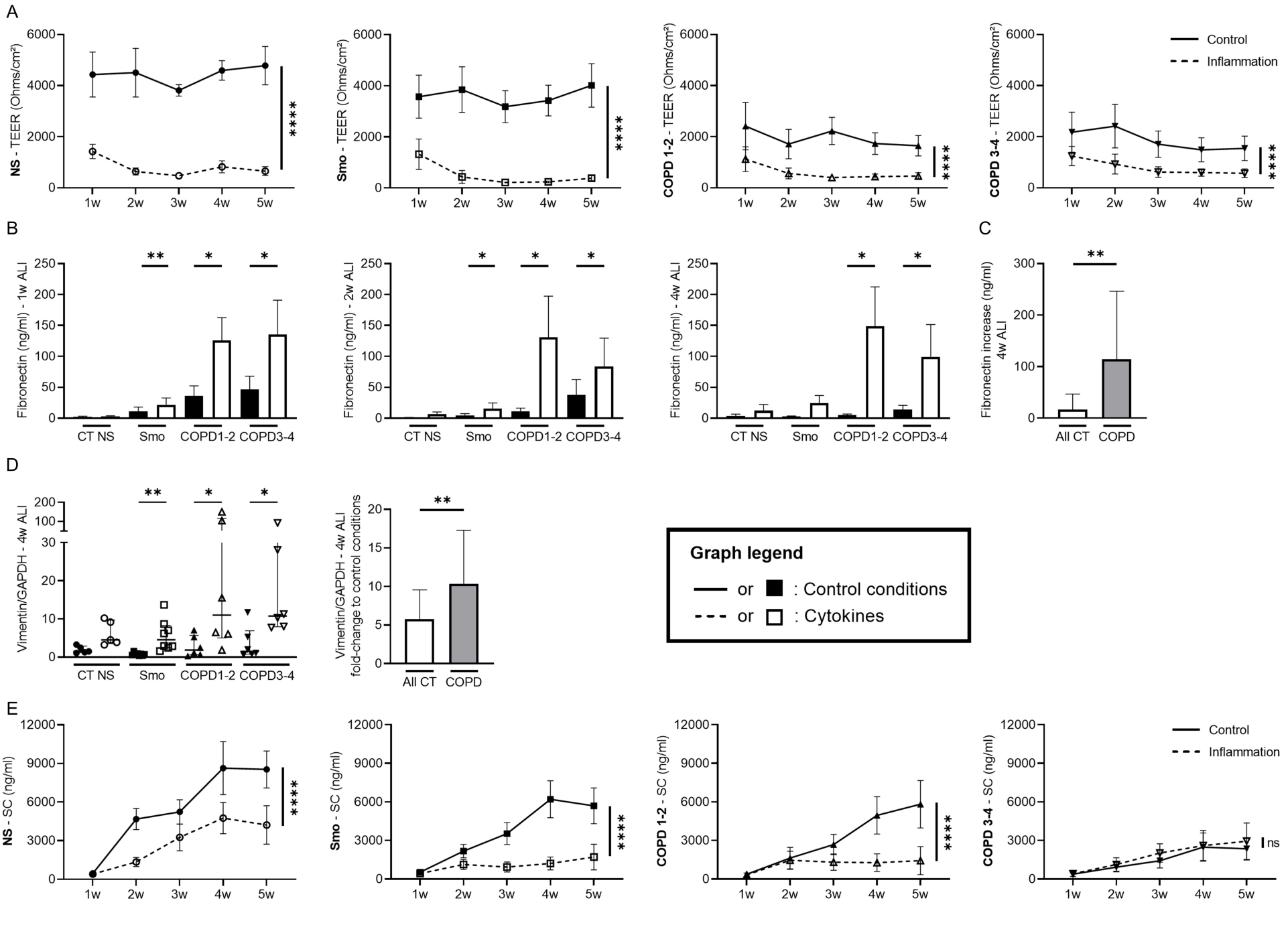
A
NS - TEER (Ohms/cm²)
Smo - TEER (Ohms/cm²)
COPD 1-2 - TEER (Ohms/cm²)
COPD 3-4 - TEER (Ohms/cm²)
Control
Inflammation
1w
2w
3w
4w
5w
****
B
Fibronectin (ng/ml) - 1w ALI
Fibronectin (ng/ml) - 2w ALI
Fibronectin (ng/ml) - 4w ALI
CT NS
Smo
COPD1-2
COPD3-4
C
Fibronectin increase (ng/ml) 4w ALI
All CT
COPD
D
Vimentin/GAPDH - 4w ALI
Vimentin/GAPDH - 4w ALI fold-change to control conditions
Graph legend
or : Control conditions
or : Cytokines
E
NS - SC (ng/ml)
Smo - SC (ng/ml)
COPD 1-2 - SC (ng/ml)
COPD 3-4 - SC (ng/ml)
ns